

## Multi-model weighting approach for future projections of solar radiation, temperature and precipitation under global warming effect in Tehran, Iran

Ehsan Mosadegh<sup>1\*</sup> and Iman Babaeian<sup>2</sup>

<sup>1</sup> PhD student, Atmospheric Sciences Department, University of Nevada, Reno, USA

<sup>2</sup> Assistant Professor, Climate Research Institute, Atmospheric Science and Meteorological Research Center, Mashhad, Iran

(Received: 18 October 2021, Accepted: 26 February 2022)

### Abstract

In order to investigate the scope of uncertainty in projections of GCMs for Tehran province, a multi-model projection composed of 15 models is employed. The projected changes in minimum temperature, maximum temperature, precipitation, and solar radiation under the A1B scenario equivalent to RCP4.5 for Tehran province are investigated for 2011-2030, 2046-2065, and 2080-2099. GCM projections for the study region are downscaled by the LARS-WG5 model. In climate change impact assessment studies, due to the influence of different sources of uncertainty on the output of the predicting system, projections do not have sufficient confidence. Therefore, it is recommended that for quantifying the range of uncertainty in the projections, the maximum number of available GCM models be used in simulations. In this regard, 15 GCMs used in this study are a subset of the CMIP4 models used in the IPCC 4th assessment report published in 2007. All these models are the coupled Atmospheric-Oceanic models and have been run for the 1960-2100 period. Uncertainty among the projections is evaluated from three perspectives: large-scale climate scenarios, downscaled values, and mean decadal changes. 15 GCMs unanimously project an increasing trend in the temperature for the study region. Also, uncertainty in the projections for the summer months is greater than projection uncertainty for other months. The mean absolute surface temperature increase for the three periods is projected to be about 0.8°C, 2.4°C, and 3.8°C in the summers, respectively. The uncertainty of the multi-model projections for precipitation in summer seasons and the radiation in the springs and falls is higher than in other seasons for the study region. Model projections indicate that for the three future periods and relative to their baseline period, springtime precipitation will decrease about 5%, 10%, and 20%, and springtime radiation will increase about 0.5%, 1.5%, and 3%, respectively. The projected mean decadal changes indicate an increase in temperature and radiation and a decrease in precipitation. Furthermore, the performance of the GCMs in simulating the baseline climate by the MOTP method does not indicate any distinct pattern among the GCMs for the study region. The future projection of temperature confirms that Tehran will experience hotter summers in the future compared to the base period. This, together with the increased sunshine in the springs and summers, can increase the frequency of temperature- and radiation-related phenomena such as photochemical pollution and may degrade the future summertime air quality in the study region. Moreover, the projected reduction in winter and spring precipitation, together with increased temperature, may increase the demands in the region.

**Keywords:** Tehran, climate change, statistical downscaling, IPCC AR4, uncertainty

---

\*Corresponding author:

emosadegh@nevada.unr.edu

## 1 Introduction

General Circulation Models (GCMs) are considered important tools for simulating the future global climate. These models are able to simulate different earth systems such as the atmosphere, oceans, and earth's surface. However, projections of these models have low confidence and high uncertainty. Therefore, in climate change studies, the Intergovernmental Panel on Climate Change (IPCC) recommends using multiple GCMs in climate simulations to consider the range of uncertainty in the projections (Parry et al., 2007). Based on this suggestion, several studies have been conducted using the multi-model ensemble approach in climate change simulations (Caballero et al., 2007; Lopez et al., 2009; Beyene et al., 2010; Hay and McCabe, 2010; Raje and Mujumdar, 2010; Setegn et al., 2011). Adopting this approach, several studies have addressed the performance of the models in simulations. Giorgi and Mearns (2002) defined 'model performance' and 'model convergence' criteria as the two validation criteria for evaluating the skill of the GCMs in simulating climate variables in the present and future climates. By these two criteria, they evaluated the performance of nine GCM models in simulating mean seasonal temperature and precipitation for 22 regions on the Earth by employing the Reliability Ensemble Averaging (REA) method. This method reduces the range of uncertainty in the simulations by minimizing the effect of the outlier models (models with weak performance). These two criteria have been addressed in several studies and with different techniques (Perkins et al., 2007; Murphy et al., 2004; Tebaldi and Knutti, 2007; Giorgi and Mearns, 2003; Tebaldi et al., 2005; Knutti et al., 2010). Perkins et al. (2007) evaluated the performance of 14 GCM models based on their skill in simulating the baseline period in 12 regions in Australia. By using the daily simulations

of precipitation, minimum temperature, and maximum temperature and calculating the probability distribution functions of the observed and simulated variables, they ranked the GCM models based on their skill in simulating the climate variables over Australia. Wilby and Harris (2006), by proposing a probabilistic structure, evaluated the impact of different uncertainty sources in simulating annual flows. In their study, they used four GCMs, two downscaling techniques, two hydrological models, and two emission scenarios, and investigated the influence of each source on output results. Moreover, Dessai and Hulme (2007), by using two GCMs investigated present uncertainty in each part of the modeling process of simulating the climate change impact on water

resources. Results of these two studies showed that if GCM variables are used as the inputs to the hydrological impact assessment models, the uncertainty of the GCM models will influence the final results, and the influence of GCMs will be greater than other sources of uncertainty. In another study, Semenov, and Stratonovitch (2010), by using a combination of outputs of fifteen GCMs and the LARS-WG statistical downscaling model, investigated the uncertainty of these models in projecting the impact of climate change on the probability of heat stress during the flowering of wheat at four European locations. Rahmani and Zarghami (2013) investigated the performance of 15 GCMs in projecting the impact of climate change on temperature and precipitation in the north-western region of Iran in the period of 2011-2030 by using the Ordered Weighted Averaging (OWA) approach. Likewise, Gohari et al. (2013) investigated the uncertainty in projecting the impact of climate change on gains and water demand by projecting the temperature and precipitation for the 2015-2044 period in the Zayanderood watershed by using

multi-model ensemble scenarios. In both studies, the LARS-WG model was used to downscale the GCM outputs.

Climate change is projected to impact each component of the climate system in all regions of the world, but with different magnitude and confidence (IPCC, 2021; Mejia et al., 2018; Mosadegh et al., 2018; Mosadegh and Nolin, 2020). A few studies have investigated climate model projections of changes in climate variables over the 21st century for the Tehran region (Mosadegh and Babaeian, 2021), and have addressed the uncertainty of these projections (Mosadegh et al., 2013), and have investigated the potential impact of the projected changes in climate variables on other aspects of the environment such as air quality (Mosadegh et al., 2022). In the present study, the range of changes in temperature, solar radiation, and precipitation under climate change in the present century has been investigated in an urban environment. For this purpose, concerning the maximum use of GCMs, projections of 15 GCMs, which were downscaled by using the LARS-WG5 stochastic weather generator for three periods of 2011-2030, 2046-2065, and 2070-2099, have been included in this study to involve the range of uncertainty of the models in projections. GCM projections were investigated based on the performance of the models in simulating the present climate (historical period) and convergence of the simulations for the three future periods. Finally, GCM simulations were evaluated to identify which model would be more skillful over the study region.

## 2 Methodology

### 2.1 Study region

*Dushan Tappeh* synoptic station is located east of Tehran at 35° 42' N, and 51° 20' E with a height of 1209.2 m above mean sea level. This station was selected due to having the longest observations in the study region, and the 1972-2009 period with

38-year daily observations was selected as the baseline period to synchronize with the historical period of GCMs. In preparing the LARS-WG input scenario file, daily observations of the baseline period are used. Therefore, observations of daily precipitation, daily minimum temperature, and daily maximum temperature for every single day of the baseline period were extracted from this station. Solar radiation was not available for the baseline period in the study region. Therefore, daily total sunshine hours were used as an alternative to the radiation input. LARS-WG uses a regression approach to convert daily sunshine hours to daily total solar radiation received by the Earth's surface at a site (Rietveld, 1978).

### 2.2 GCMs and emission scenarios

Currently, the main and the most powerful tools for global climate change projections are the GCMs (Giorgi and Francisco, 2001; Lane et al., 1999; Mitchell, 2003). These models are based on physical concepts defined by mathematical equations solved on a three-dimensional grid on the Earth. 15 GCMs used in this study are a subset of the models which are used in the IPCC 4<sup>th</sup> assessment report which was published in 2007. All these models are the coupled Atmospheric-Oceanic models, and most of them have been run for the 1960-2100 period. Features of these 15 models are presented in table 1. For simulating the future climate, the models consider an estimate of future emissions of greenhouse gases as their input. These estimates are called emission scenarios, which consider a wide range of effective factors such as future human population, and economic and technological factors affecting emissions of greenhouse gases and aerosols. In this study, A1B emission scenarios equivalent to RCP4.5 from among SRES scenarios are used. This scenario is considered a moderate scenario, and most of the GCMs have used this scenario in their climate simulations.

### 2.3 Downscaling

In this study, the LARS-WG5 model was used to downscale the GCM simulations. LARS-WG is a statistical downscaling model placed among stochastic weather generator tools. Weather generators can simulate statistical characteristics of local climate variables and generate local-scale daily climate scenarios for a specific station (Wilby et al., 2004). First, in the calibration step, the model extracts the statistical characteristics of each variable from long-term baseline observations and, by using these characteristics, regenerates the probability distribution of the variables for the baseline period. Then, in the quality test step, the model compares the statistical characteristics of the generated and observed variables in each month, assuming that the observations are a random sample from the existing sample which is considered as the true climate at the site. The comparison of the generated and observed data is done by performing some statistical tests such as t, F, and K-S tests, which are for comparing means, standard deviations, and probability distributions of the two data sets, respectively. Each test delivers test statistics and p-values for each month. The p-value is computed at the 0.05 significance level, and the values above this level indicate the high probability of simi-

larity between the two data sets. Eventually, in the final step, using the calculated statistical characteristics of the local climate and GCM climate scenarios for the study grid, daily time series of each variable is generated for the desired period in the future (Semenov and Barrow 2002).

### 2.4 Uncertainty in climate modeling

Studies show that GCMs provide a realistic projection of the future climate (Solomon et al., 2007). The ability of GCMs to reproduce a broad range of climate attributes increases the confidence of climate scientists that key physical processes are included in climate change simulations (Doblas-Reyes et al., 2006; Palmer et al., 2004; Palmer et al., 2005). However, in climate change studies and in different parts of simulating the climate variables, different sources of uncertainty exist that can influence the final output of the study. Giorgi and Francisco (2001) showed that the main sources of uncertainty in climate change simulations on a regional scale stem from uncertainty in greenhouse gas emission scenarios, uncertainty in GCM simulations and their internal differences, and uncertainties in different methods of downscaling GCM simulations. Furthermore, Wilby and Harris (2006) and Dessai and Hulme (2007) showed that GCM

**Table 1:** Features of the GCMs from IPCC AR4 used in this study

Country	Developer	GCM	Model acronym	Grid resolution	Emission scenarios
Australia	Commonwealth Scientific and Industrial Research Organization	CSIRO-MK3.0	CSMK3	1.9° × 1.9°	SRA1B, SRB1
Canada	Canadian Centre for Climate Modeling and Analysis	CGCM33.1 (T47)	CGMR	2.8° × 2.8°	SRA1B
China	Institute of Atmospheric Physics	FGOALS-g1.0	FGOALS	2.8° × 2.8°	SRA1B, SRB1
France	Centre National de Recherches Meteorologiques	CNRM-CM3	CNCM3	1.9° × 1.9°	SRA1B, SRA2
France	Institute Pierre Simon Laplace	IPSL-CM4	IPCM4	2.5° × 3.75°	SRA1B, SRB1, SRA2
Germany	Max-Planck Institute for Meteorology	ECHAM5-OM	MPEH5	1.9° × 1.9°	SRA1B, SRB1, SRA2
Japan	National Institute for Environmental Studies	MRI-CGCM2.3.2	MIHR	2.8° × 2.8°	SRA1B, SRB1
Norway	Bjerknes Centre for Climate Research	BCM2.0	BCM2	1.9° × 1.9°	SRA1B, SRB1
Russia	Institute for Numerical Mathematics	INM-CM3.0	INCM3	4° × 5°	SRA1B, SRB1, SRA2
UK	UK Meteorological Office	HadCM3	HADCM3	2.5° × 3.75°	SRA1B, SRB1, SRA2
		HadGEM1	HADGEM	1.3° × 1.9°	SRA1B, SRA2
USA	Geophysical Fluid Dynamics Lab	GFDL-CM2.1	GFCM21	2.0° × 2.5°	SRA1B, SRB1, SRA2
USA	Goddard Institute for Space Studies	GISS-AOM	GIAOM	3° × 4°	SRA1B, SRB1
USA	National Centre for Atmospheric Research	PCM	NCPCM	2.8° × 2.8°	SRA1B, SRB1
		CCSM3	NCCCS	1.4° × 1.4°	SRA1B, SRB1, SRA2

models have the highest uncertainty compared to other components of hydrological impact assessment systems.

Intercomparison studies of GCMs indicate that climate variables are simulated with different degrees of accuracy by different models, and no single model delivers the best simulation for all variables and/or all regions (Lambert and Boer, 2001; Gleckler et al., 2008). Furthermore, in climate change impact assessment studies, due to the influence of different sources of uncertainty on the output of the predicting system, projections do not have sufficient confidence. Therefore, it is recommended that for quantifying the range of uncertainty in the projections, the maximum number of available GCM models be used in simulations (Jones, 2000; Wilby and Harris, 2006). Lambert and Boer (2001) and Gleckler et al. (2008) showed that the multi-model mean of an ensemble simulation yields a closer estimate of reality. Giorgi and Mearns (2002) defined two “*reliability criteria*” for evaluating the performance of GCMs in simulations: the ‘model performance’ criterion, which means how well the models can simulate the baseline (present) climate, and the ‘model convergence’ criterion, which investigates the convergence between the simulations of future climate across the models. By considering both these criteria, they investigated the accuracy of the models in simulating the mean seasonal changes of temperature and precipitation simulated by 9 GCMs over 22 regions of the world. They assigned weights to the calculated means of each GCM and calculated the weighted mean of the variables among the GCMs projections. However, Christensen et al. (2010) showed that averaging the weighted simulations in a multi-model projection is not superior to an unweighted mean, and weighting the models incorporates a level of uncertainty to ensemble-based climate simulations.

#### 2.4.1 Performance of GCMs in simulating mean climate

To investigate which GCM can generate closer simulations for the study region (performance criterion in GCMs), the Mean Observation Temperature Precipitation (MOTP) method was used to assign weights to each GCM based on the deviation of its baseline simulated mean temperature (or precipitation) from its mean observation values using the Eq. 1 (Gohari et al., 2013)

$$W_{ij} = \frac{\frac{1}{\Delta_{ij}}}{\sum_{j=1}^n \frac{1}{\Delta_{ij}}} \quad (1)$$

where  $W_{ij}$  is the weight of the GCM  $j$  in month  $i$ ,  $n$  is the number of total GCMs, and  $\Delta_{ij}$  is the difference between the simulated mean temperature or precipitation and its corresponding observed value by GCM  $j$  in a month  $i$  in the baseline period. The GCM simulations over the study region for the observation period were obtained from the Canadian climate change database (<http://www.cccsn.ec.gc.ca>), and then the monthly means were calculated for each GCM in the baseline period.

#### 2.4.2 Range of uncertainty in projections

In the present study, to investigate the convergence criterion, simulations of precipitation, minimum temperature, maximum temperature, and solar radiation by 15 GCMs are illustrated in box plots. In this method, all the simulations conducted by the 15 GCMs for the study region in each month are illustrated in a single figure. Therefore, it enables the reader to easily compare the present range of uncertainty and its change over the different periods in the simulations. In figures 2-5, the bottom and top borders of each box demonstrate the first and third quartile of the simulations, and the bottom and top lines out of the boxes demonstrate the minimum and the maximum of the projections, respectively. The middle line on the boxes also

demonstrates the median of the simulations. Moreover, the unweighted means of the simulations of the 15 GCMs are illustrated on each box. It is noteworthy that the box plot does not illustrate a certain range of changes in simulations but shows the range of uncertainty from the perspective of the employed GCMs in the simulations.

### 3 Results and discussion

#### 3.1 Validation of LARS-WG

Comparison of monthly means and standard deviations of the simulated and observed variables at the *Dushan Tappeh* station for the baseline period (1972-2009) is illustrated in Figure. 1. As the figure shows, in March and December, LARS-WG has the highest error in simulating the monthly means of precipitation, which is about 6.5 mm wet bias. In simulating the monthly means of minimum and maximum temperature, the difference is negligible. The greatest difference in simulating the mean minimum temperature is in November, which is about 0.4 °C lower than the observations, and the maximum temperature is in October and December, which is about 0.4 °C. In simulating the radiation, the greatest difference is in November and about 0.4 Mj/m<sup>2</sup>.day lower than the observations.

Moreover, the generated monthly means were compared with their corresponding observations in the baseline period by the t-test. For every month, the test results were evaluated at the 0.05 confidence level. The test statistics and p-values for each variable in each month are given in table 2. The test results show that the simulated monthly means of all variables in all months are similar to their corresponding observations. Except for the monthly simulated radiation in November, simulations of all the four climate variables in all months are acceptable at the 0.05 confidence level.

#### 3.2 Climate scenarios

Box plot was used to illustrate and analyze the range of uncertainty in the large-scale climate change scenarios projected by 15 GCMs for the study region. For plotting each box, projections of the 15 GCMs for each climate variable in each period were used. Moreover, to compare the changes in each period, the unweighted means of the 15 projections in each month are illustrated with bars on each box. In addition, to compare the future changes with the baseline period, diagrams of the long-term monthly means of each variable in the baseline period are shown on the boxes. Figures. 2 and 3 illustrate the projected absolute changes in the minimum and maximum temperature in projecting the temperature in the summers than in other seasons. The convergence in the projections will also reduce in the long term in all months of the year.

The mean absolute temperature increase under the A1B emission scenario is projected to be about 0.8 °C, 2.4 °C, and 3.8 °C in the summers, and about 0.5 °C, 1.5 °C, and 2.3 °C in the winters for the three periods, respectively. Figures. 4 and 5 illustrate the relative changes in the precipitation and solar radiation in percent, projected by 15 GCMs for the three future periods relative to their baseline period for each month of the year, respectively. The figures show that the changes in the two variables have almost a reverse pattern so that the models project decreased precipitation and increased solar radiation for the springs but increased precipitation and decreased radiation for the falls. The decrease in precipitation in the springs may be due to the reduced cloudiness and increased radiation in the season, which this trend will be reversed in the falls. Moreover, the projections state that the relative reduction in the precipitation reaches its peak in summers (June, July, and August), but because the precipitation and the cloudiness in this season are less than in other seasons, no great changes in the amount of received radiation are projected

for the summers.

Furthermore, the models project the least convergence and the most uncertainty in relative changes in the precipitation for the summers and as a reduction in precipitation. However, due to the small amount of precipitation in this season, this reduction will not have a great effect on the amount of precipitation received by the Earth's surface. This reduction will be more pronounced in the winters, which have a high amount of precipitation. It is projected that, relative to the baseline pe-

riod, the winter precipitation will be reduced on average by about 2%, 8%, and 15% from the first to the third period, respectively. In terms of solar radiation, the models show the highest uncertainty in the projected relative changes in radiation for the springs and then falls, and as an increase and a decrease in the radiation, respectively. It is projected that, relative to the baseline period, the spring radiation will be increased on average about 0.5%, 1.5%, and 3% from the first to the third period, respectively.

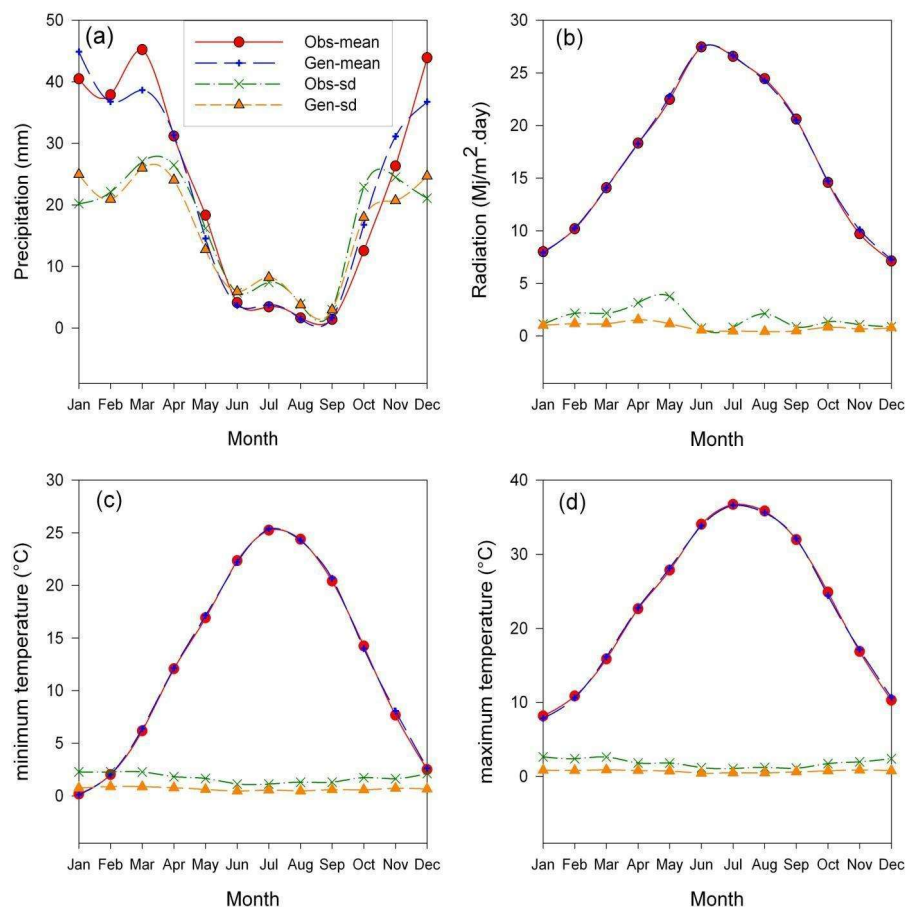


**Figure 1.** Comparison of monthly means and standard deviations of the simulated and observed variables at the *Dushan Tappeh* station in the baseline period (1972-2009) for (a) precipitation (mm), (b) radiation (MJ/m<sup>2</sup>.day), (c) minimum temperature (°C), and (d) maximum temperature (°C).

### 3.3 Downscaling GCM outputs

Projections of the 15 GCMs were downscaled for the study region and local-scale daily climate scenarios of the variables were obtained for each period.

For investigating the convergence across the projections after the downscaling, all downscaled daily values of each variable in each month are gathered in one box. To compare the range of uncertainty entered

to the projections after the downscaling, the changes in large-scale climate scenarios are also illustrated in Figure. 6. Figure. 6 shows this comparison for the maximum temperature. The small boxes on the left in each month are formed by adding the projected absolute temperature increase to the long-term observed monthly means of the baseline maximum temperature.

The boxes on the right for each month show the range of the downscaled daily maximum temperature obtained from all downscaled daily values from LARS-WG for each month in each period. The baseline long-term monthly means of the

maximum temperature are also illustrated under the boxes. Figure. 6 shows that the changes in both diagrams follow the same trend. All diagrams show the temperature rise relative to the long-term baseline means, and this increase has grown by the end of the 21<sup>st</sup> century. However, a noticeable difference exists between the ranges of changes in the maximum temperature in the 2 sets of changes in both diagrams follow the same trend. All diagrams show the temperature rise relative to the long-term baseline means, and this increase has grown by the end of the 21<sup>st</sup> century.

**Table 2.** Statistical tests and their p-values from LARS-WG

Month	Precipitation				Minimum temperature				Maximum temperature				Solar radiation			
	K-S	P-Value	t	P-Value	K-S	P-Value	t	P-Value	K-S	P-Value	t	P-Value	K-S	P-Value	t	P-Value
Jan	0.058	1	-0.87	0.385	0.106	0.9989	0.147	0.883	0.106	0.9989	0.697	0.488	0.044	1	0.363	0.718
Feb	0.04	1	0.234	0.816	0.053	1	-0.08	0.936	0.105	0.9991	0.63	0.531	0.087	1	-0.18	0.851
Mar	0.136	0.9743	1.124	0.264	0.053	1	-0.56	0.573	0.053	1	-0.76	0.45	0.087	1	0.016	0.987
Apr	0.069	1	-0.03	0.971	0.106	0.9989	-0.25	0.801	0.053	1	-0.41	0.678	0.044	1	0.079	0.937
May	0.084	1	1.196	0.235	0.053	1	-0.90	0.366	0.053	1	-1.05	0.297	0.087	1	-0.56	0.572
Jun	0.131	0.9824	0.333	0.74	0.106	0.9989	0.761	0.449	0.106	0.9989	0.977	0.331	0.044	1	-0.02	0.978
Jul	0.117	0.9954	-0.18	0.857	0.105	0.9991	-0.67	0.503	0.105	0.9991	0.601	0.549	0.044	1	-0.59	0.552
Aug	0.305	0.1932	0.255	0.799	0.106	0.9989	0.414	0.68	0.106	0.9989	1.032	0.305	0.131	0.9824	0.547	0.586
Sep	0.29	0.2415	-0.47	0.638	0.053	1	-1.18	0.238	0.053	1	-0.81	0.419	0.087	1	0.778	0.439
Oct	0.057	1	-0.95	0.342	0.105	0.9991	0.858	0.393	0.106	0.9989	1.509	0.135	0.044	1	-0.55	0.584
Nov	0.088	1	-0.97	0.331	0.053	1	-1.51	0.134	0.053	1	-0.89	0.375	0.044	1	-1.99	0.05
Dec	0.042	1	1.412	0.162	0.105	0.9991	-0.4	0.69	0.053	1	-1.02	0.307	0.131	0.9824	-0.71	0.477

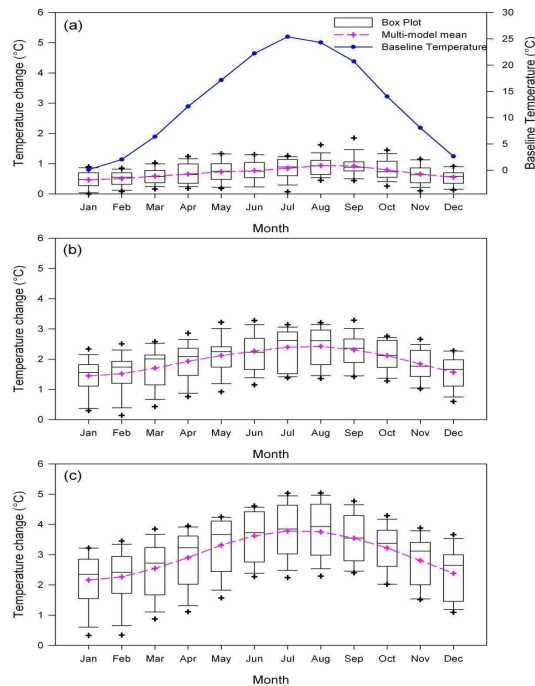


**Figure 2.** Projected absolute changes in the minimum surface temperature (°C) relative to the baseline period (1972-2009) at the Dushan Tappeh station for the three periods: (a) 2011-2030, (b) 2046-2065, and (c) 2080-2099.



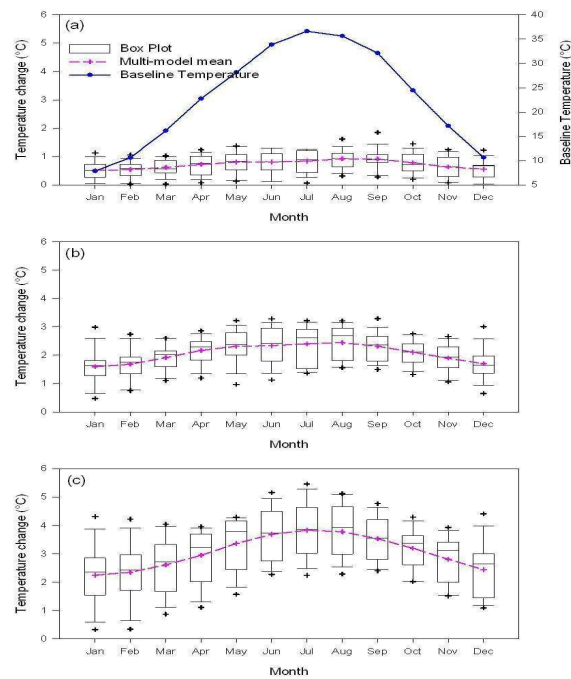


**Figure 3.** Projected absolute changes in the maximum surface temperature ( $^{\circ}\text{C}$ ) relative to the baseline period (1972-2009) at the Dushan Tappeh station for the three periods: (a) 2011-2030, (b) 2046-2065, and (c) 2080-2099.

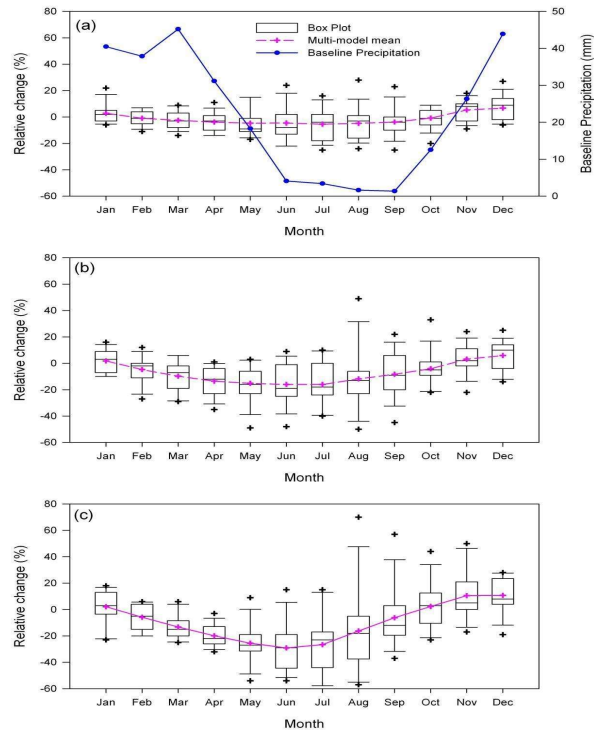


**Figure 4.** Projected relative changes in precipitation relative to the baseline period (1972-2009) at the *Dushan Tappeh* station for the three periods: (a) 2011-2030, (b) 2046-2065, and (c) 2080-2099.

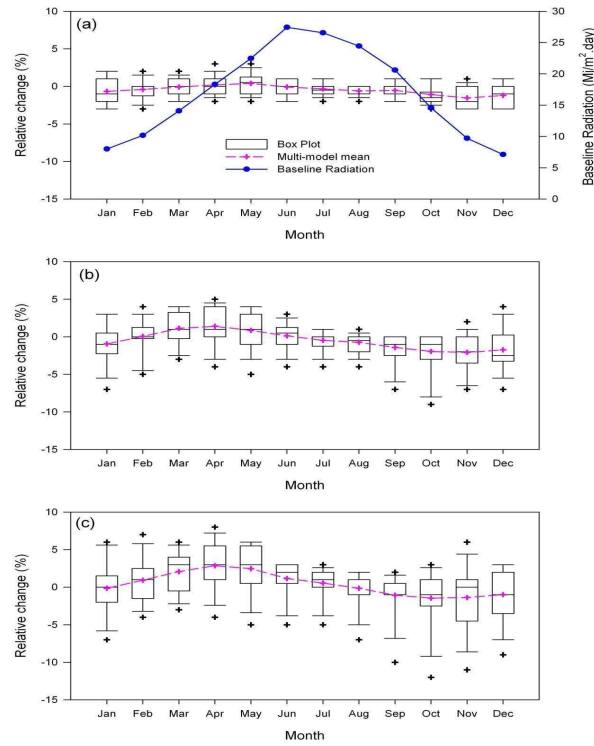


**Figure 5.** Projected relative changes in solar radiation relative to the baseline period (1972-2009) at the Dushan Tappeh station for the three periods: (a) 2011-2030, (b) 2046-2065, and (c) 2080-2099.

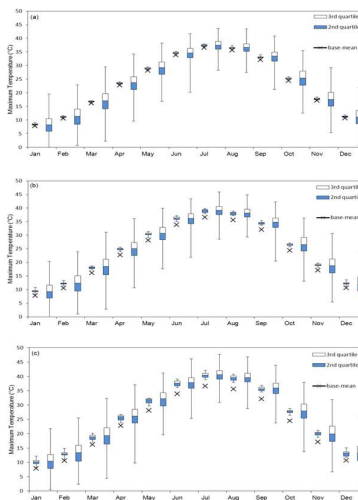


**Figure 6.** Comparison of convergence between daily values (downscaled by LARS-WG, large boxes) and large-scale climate scenarios (GCM outputs, small boxes) for the maximum temperature at the Dushan Tappeh station for the three periods: (a) 2011-2030, (b) 2046-2065, and (c) 2080-2099.

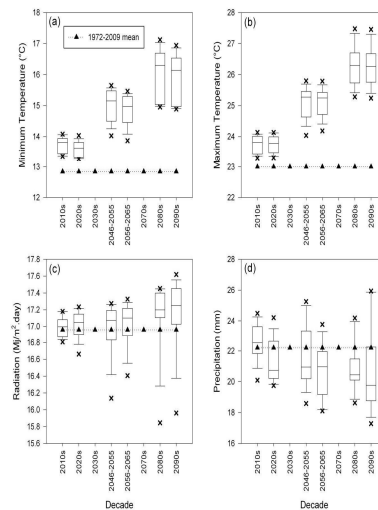


**Figure 7.** Projections of the mean decadal changes of (a) minimum temperature, (b) maximum temperature, (c) solar radiation, and (d) precipitation under the influence of climate change for the Dushan Tappeh station.

However, a noticeable difference exists between the ranges of changes in the maximum temperature in the 2 sets of diagrams in each period. The downscaled values have a wider range compared to the large-scale projections. This increase in the range can result from the increase in climate fluctuations due to downscaling the variables from the grid scale to the local scale (study station). Furthermore, a comparison of the three periods ((a) 2011-2030, (b) 2046-2065, and (c) 2080-2099) in Figure. 6 shows that the convergence in the projected large-scale climate scenarios (small boxes) in the summers is less than in other seasons, but after the downscaling, the convergence in the projections in the summers is more than other seasons.

### 3.4 Mean decadal changes of the climate variables for the *Dushan Tappeh* station

Changes in the climate variables in the future decades under the influence of climate change were also investigated from the mean decadal perspective. For each GCM, the decadal means of radiation, minimum and maximum temperature were obtained from averaging the downscaled daily values of each variable

in each decade. For calculating the decadal mean of precipitation projected by each GCM, initially, monthly total precipitation was calculated from daily values and then the mean monthly total precipitation was calculated for each decade. Each box in Figure. 7 illustrates the projections of the 15 GCMs compared to the baseline long-term means of each variable. The ensemble projections indicate that the decadal changes of radiation, minimum, and maximum temperature will have an increasing trend, while the decadal changes of precipitation will have a decreasing trend in the coming decades. Decadal changes of the minimum and maximum temperature show a more distinct trend in comparison with the decadal changes of precipitation and radiation, and all GCMs unanimously project a noticeable growth in decadal changes of temperature. The figure indicates that the convergence in the projections reduces in the long term in all variables. Furthermore, the models project a reverse pattern for changes in radiation and precipitation in the future decades. The ensemble projections indicate that in the long term, precipitation will decrease, and in contrast, the radiation will increase in the study region.

### 3.5 Weighting of the models

Studies indicate that the skills of GCMs in simulating all climate variables are not similar, and the accuracy of GCMs projections is different for different variables and/or regions (Gleckler et al., 2008). Therefore, the weighting of the projections by 15 GCMs for the study region was conducted by the MOTP method to investigate which GCM demonstrates better performance in simulating the baseline climate. Table 3 shows that weighting the simulated monthly means of the variables do not show a distinct pattern, but it seems that in simulating the maximum temperature, MIHR, and CSMK3 show a better performance in the warm and cold months, respectively. In simulating the

minimum temperature, CSMK3, FGOALS, and IPCM4 perform better in the simulations in the first four months, second 4 months, and the last four months of the year, respectively.

In simulating the daily mean temperature, no distinct pattern can be seen among the simulations, and only the CSMK3 shows a better performance in simulating the daily mean temperature for the first 4 months of the year. In simulating the precipitation, similar to the daily mean temperature, no distinct pattern can be seen among the models, although it seems that NCCCSM shows a better performance in simulating the precipitation in some months for the study region.

**Table 3.** Relative weights of the GCMs in simulating the monthly means of the variables: (a) daily maximum temperature (°C), (b) daily minimum temperature (°C), (c) daily mean temperature (°C), and (d) daily precipitation (mm/day).

**(a)**

Month	BCM2	CGMR	CNCM3	CSMK.3	FGOALS	GFCM21	GIAOM	HADCM3	HADGEM	INCM3	IPCM4	MIHR	MPEH5	NCCCSM	NCPCM
Jan	0.02	0.05	0.03	0.23	0.03	0.33	0.09			0.11	0.07	0.04			
Feb	0.02	0.04	0.03	0.49	0.03	0.15	0.06			0.1	0.05	0.04			
Mar	0.02	0.05	0.04	0.57	0.04	0.08	0.04			0.08	0.04	0.05			
Apr	0.05	0.11	0.1	0.15	0.09	0.11	0.06			0.12	0.08	0.14			
May	0.03	0.12	0.06	0.08	0.07	0.07	0.03			0.06	0.04	0.43			
Jun	0.04	0.11	0.07	0.09	0.13	0.15	0.06			0.07	0.06	0.23			
Jul	0.04	0.04	0.11	0.06	0.15	0.34	0.06			0.05	0.04	0.12			
Aug	0.04	0.05	0.07	0.05	0.08	0.25	0.06			0.05	0.05	0.29			
Sep	0.04	0.15	0.07	0.05	0.06	0.15	0.07			0.06	0.06	0.29			
Oct	0.01	0.64	0.02	0.02	0.02	0.03	0.02			0.02	0.02	0.19			
Nov	0.05	0.11	0.07	0.11	0.06	0.11	0.09			0.09	0.18	0.12			
Dec	0.04	0.07	0.05	0.14	0.05	0.16	0.1			0.09	0.25	0.07			

**(b)**

Month	BCM2	CGMR	CNCM3	CSMK.3	FGOALS	GFCM21	GIAOM	HADCM3	HADGEM	INCM3	IPCM4	MIHR	MPEH5	NCCCSM	NCPCM
Jan	0.02	0.02	0.03	0.53	0.02	0.05	0.09			0.03	0.19	0.03			
Feb	0.02	0.03	0.04	0.48	0.03	0.06	0.09			0.03	0.18	0.04			
Mar	0.05	0.06	0.07	0.28	0.07	0.09	0.11			0.06	0.14	0.07			
Apr	0.07	0.07	0.08	0.17	0.14	0.1	0.1			0.06	0.13	0.08			
May	0.07	0.07	0.09	0.14	0.17	0.09	0.09			0.06	0.13	0.09			
Jun	0.07	0.07	0.08	0.1	0.27	0.07	0.08			0.05	0.13	0.08			
Jul	0.06	0.07	0.07	0.07	0.38	0.06	0.07			0.04	0.12	0.07			
Aug	0.07	0.08	0.08	0.09	0.22	0.07	0.09			0.05	0.16	0.09			
Sep	0.07	0.08	0.09	0.09	0.15	0.08	0.1			0.05	0.21	0.09			
Oct	0.07	0.07	0.08	0.1	0.12	0.08	0.09			0.05	0.24	0.1			
Nov	0.05	0.05	0.05	0.09	0.06	0.06	0.07			0.04	0.48	0.06			
Dec	0.05	0.04	0.05	0.21	0.05	0.07	0.09			0.04	0.33	0.06			

(c)

Month	BCM2	CGMR	CNCM3	CSMK.3	FGOALS	GFCM21	GIAOM	HADCM3	HADGEM	INCM3	IPCM4	MIHR	MPEH5	NCCCSM	NCPCM
Jan	0.02	0.03	0.02	0.4	0.02	0.08	0.07	0.03	0.03	0.04	0.12	0.03	0.04	0.04	0.02
Feb	0.02	0.03	0.03	0.44	0.03	0.08	0.07	0.03	0.03	0.05	0.07	0.04	0.04	0.03	0.02
Mar	0.03	0.05	0.05	0.31	0.05	0.08	0.06	0.04	0.04	0.06	0.07	0.06	0.04	0.04	0.03
Apr	0.05	0.07	0.07	0.13	0.09	0.08	0.06	0.04	0.04	0.06	0.09	0.08	0.05	0.04	0.04
May	0.05	0.08	0.08	0.11	0.12	0.08	0.06	0.04	0.03	0.06	0.08	0.13	0.04	0.04	0.03
Jun	0.05	0.15	0.06	0.08	0.16	0.07	0.06	0.03	0.02	0.04	0.07	0.12	0.03	0.03	0.02
Jul	0.04	0.3	0.05	0.05	0.19	0.06	0.05	0.02	0.02	0.03	0.05	0.11	0.02	0.02	0.02
Aug	0.05	0.21	0.07	0.06	0.13	0.07	0.07	0.02	0.02	0.04	0.08	0.12	0.03	0.03	0.02
Sep	0.06	0.14	0.07	0.06	0.1	0.08	0.08	0.03	0.03	0.05	0.11	0.1	0.03	0.03	0.03
Oct	0.05	0.1	0.06	0.08	0.07	0.08	0.07	0.04	0.04	0.05	0.12	0.13	0.04	0.04	0.03
Nov	0.05	0.06	0.05	0.09	0.05	0.07	0.07	0.04	0.05	0.05	0.22	0.08	0.05	0.05	0.03
Dec	0.02	0.02	0.02	0.08	0.02	0.05	0.04	0.02	0.03	0.03	0.56	0.03	0.03	0.03	0.02

(d)

Month	BCM2	CGMR	CNCM3	CSMK.3	FGOALS	GFCM21	GIAOM	HADCM3	HADGEM	INCM3	IPCM4	MIHR	MPEH5	NCCCSM	NCPCM
Jan	0.07	0.02	0.01	0.01	0.02	0.01	0.02	0.01	0.08	0.01	0.19	0.04	0.01	0.48	0.01
Feb	0.01	0.04	0.74	0.01	0.03	0.03	0.01	0.01	0.01	0.01	0.03	0.03	0.01	0.02	0.01
Mar	0.01	0.15	0.01	0.02	0.13	0.09	0.01	0.03	0.02	0.02	0.06	0.07	0.03	0.33	0.01
Apr	0	0.01	0	0.02	0.01	0.01	0	0.05	0	0.22	0.06	0.08	0.26	0.22	0.04
May	0	0.01	0.01	0.03	0.02	0.14	0.01	0.06	0.01	0.02	0.19	0.11	0.06	0.17	0.17
Jun	0	0.02	0	0.1	0.01	0.07	0.02	0.08	0.02	0.01	0.05	0.09	0.01	0.14	0.39
Jul	0.01	0.18	0.01	0.04	0.14	0.03	0.07	0.14	0.01	0.01	0.05	0.04	0.01	0.19	0.05
Aug	0.01	0.44	0	0.04	0.09	0.05	0.05	0.13	0	0.01	0.05	0.05	0.01	0.02	0.07
Sep	0.01	0.04	0	0.01	0.03	0.47	0.01	0.02	0	0.01	0.04	0.09	0.01	0.01	0.23
Oct	0.02	0.17	0.01	0.04	0.1	0.13	0.01	0.09	0.01	0.07	0.05	0.15	0.03	0.04	0.08
Nov	0	0.02	0.02	0.07	0.09	0.22	0.02	0.05	0.02	0.16	0.16	0.07	0.04	0.03	0.03
Dec	0.08	0.04	0.03	0.03	0.04	0.03	0.07	0.02	0.08	0.03	0.06	0.07	0.03	0.38	0.02

#### 4 Conclusion

In the present study, the uncertainty of 15 GCMs in projecting the changes in temperature, precipitation, and radiation for the present century under the influence of climate change was investigated in Tehran province. All models unanimously project an increase in temperature in all months, and this increase is projected with more uncertainty for the summer seasons. The projections indicate a reverse pattern for the precipitation and radiation, showing a reduction in precipitation and an increase in the radiation are projected for the springs. Projections show that this pattern will reverse for the falls. Moreover, the convergence of the ensemble projections for precipitation in the summers, and the radiation in the springs and falls are less than other seasons for the study region. The uncertainty in the projections of the

variables also grows in the long term (by the end of the 21<sup>st</sup> century), which indicates the weakness of the GCMs in long-term climate projections. Furthermore, decadal changes in the variables indicate that temperature and radiation will increase, precipitation will decrease in the long term, and these changes are more pronounced for the temperature.

The projected changes in the climatic variables can influence the future urban environment of the study region. The projections indicate that Tehran will experience hotter summers in the future. This, together with the increased sunshine in the springs and summers, can influence temperature-related phenomena such as photochemical pollution and may degrade the future summertime air quality in the study region. Moreover, the projected reduction in winter and spring precipitation, which

has the most precipitation among other seasons, may influence the local water resources and lead to water shortage in the study region. Therefore, the consequence of the projected changes in the future climate of the study region, which is considered as the first step among the steps of climate change impact assessment, can be investigated in other environmental aspects such as air quality and water resources in the study region to evaluate the scope of the impact of these changes on other resources and to devise a mitigation and adaptation strategy for the future decades. Therefore, future work should benefit greatly from techniques such as using dynamical-regional downscaling techniques, employing more local stations, and employing impact assessment models.

#### **Acknowledgment:**

The authors would like to give special thanks to Iran Meteorological Organization for providing meteorological data used in the current study. We are also grateful to the National Climatological Research Institute of Mashhad for its contribution to this paper.

#### **References:**

- Beyene, T., Lettenmaier, D.P., Kabat, P., 2010, Hydrologic impacts of climate change on the Nile River Basin: implications of the 2007 IPCC scenarios: *Climatic Change*, 100(3):433–61.
- Caballero, Y., Voirin-Morel, S., Habets, F., Noilhan, J., LeMoigne, P., Lelienaff, A., Boone, A., 2007, Hydrological sensitivity of the Adour-Garonne river basin to climate change: *Water Resources Research*, 43(7). Available from: <https://onlinelibrary.wiley.com/doi/abs/10.1029/2005WR004192>
- Christensen, J.H., Kjellström, E., Giorgi, F., Lenderink, G., Rummukainen, M., 2010, Weight assignment in regional climate models: *Climate Research*, 44(2–3), 179–94.
- Dessai, S., Hulme, M., 2007, Assessing the robustness of adaptation decisions to climate change uncertainties: A case study on water resources management in the East of England: *Global Environmental Change*. 17(1), 59–72.
- Doblas-Reyes, F.J., Hagedorn, R., Palmer, T.N., 2006, Developments in dynamical seasonal forecasting relevant to agricultural management: *Climate Research*, 33(1):19–26.
- Giorgi, F., Francisco, R., 2001, Uncertainties in the Prediction of Regional Climate Change. In: Visconti, G., Beniston, M., Iannorelli, E.D., Barba, D. (eds) *Global Change and Protected Areas, Advances in Global Change Research*, vol 9. Springer, Dordrecht. [https://doi.org/10.1007/0-306-48051-4\\_14](https://doi.org/10.1007/0-306-48051-4_14).
- Giorgi, F., Mearns, L.O., 2002, Calculation of Average, Uncertainty Range, and Reliability of Regional Climate Changes from AOGCM Simulations via the “Reliability Ensemble Averaging” (REA) Method: *Journal of Climate*, 15(10), 1141–58.
- Giorgi, F., Mearns, L.O., 2003, Probability of regional climate change based on the Reliability Ensemble Averaging (REA) method: *Geophysical Research Letters*, 30(12). Available from: <https://onlinelibrary.wiley.com/doi/abs/10.1029/2003GL017130>
- Gleckler, P.J., Taylor, K.E., Doutriaux, C., 2008, Performance metrics for climate models: *Journal of Geophysical Research: Atmospheres*, 113(D6). Available from: <https://onlinelibrary.wiley.com/doi/abs/10.1029/2007JD008972>
- Gohari, A., Eslamian, S., Abedi-Koupaei, J., Massah Bavani, A., Wang, D., Madani, K., 2013, Climate change impacts on crop production in Iran’s Zayandeh-Rud River Basin: *Science of The Total Environment*. 442C(4), 405–

- 19.
- Hay, L.E., McCabe, G.J., 2010, Hydrologic effects of climate change in the Yukon River Basin: *Climatic Change*, 100(3), 509–23.
- IPCC, 2021: Summary for Policymakers. In: *Climate Change 2021: The Physical Science Basis. Contribution of Working Group I to the Sixth Assessment Report of the Intergovernmental Panel on Climate Change* [Masson-Delmotte, V., P. Zhai, A. Pirani, S. L. Connors, C. Péan, S. Berger, N. Caud, Y. Chen, L. Goldfarb, M. I. Gomis, M. Huang, K. Leitzell, E. Lonnoy, J.B.R. Matthews, T. K. Maycock, T. Waterfield, O. Yelekçi, R. Yu and B. Zhou (eds.)]. Cambridge University Press. In Press.
- Jones, R.N., 2000, Managing Uncertainty in Climate Change Projections – Issues for Impact Assessment: *Climatic Change*, 45(3), 403–19.
- Knutti, R., Furrer, R., Tebaldi, C., Cermak, J., Meehl, A., 2010, Challenges in combining projections from multiple climate models: *Journal of Climate*, 2739–58.
- Lambert, S.J., Boer, G.J., 2001, CMIP1 evaluation and intercomparison of coupled climate models: *Climate Dynamics*, 17, 83–106.
- Lane, M.E., Kirshen, P.H., Vogel, R.M., 1999, Indicators of Impacts of Global Climate Change on U.S. Water Resources: *Journal of Water Resources Planning and Management*, 125(4), 194–204.
- Lopez, A., Fung, F., New, M., Watts, G., Weston, A., Wilby, R.L., 2009, From climate model ensembles to climate change impacts and adaptation: A case study of water resource management in the southwest of England: *Water Resources Research*, 45(8). Available from: <https://onlinelibrary.wiley.com/doi/abs/10.1029/2008WR007499>
- Mejia, J., Wilcox, E., Rayne, S., Mosadegh, E., 2018, Final report: Vehicle Miles Traveled Review. <https://doi.org/10.13140/RG.2.2.29814.52807>
- Mitchell, T.D., 2003, Pattern Scaling: An Examination of the Accuracy of the Technique for Describing Future Climates: *Climatic Change*, 60(3), 217–42.
- Mosadegh, E., Ashrafi, K., Motlagh, M. S., Babaeian, I., 2022, Modeling the Regional Effects of Climate Change on Future Urban Ozone Air Quality in Tehran, Iran, arXiv:2109.04644, arXiv e-prints. <https://doi.org/10.48550/arXiv.2109.04644>
- Mosadegh, E., Babaeian, I., Baygi, M., 2013, Uncertainty Assessment of GCM Models in Predicting Temperature, Precipitation and Solar Radiation Under Climate Change Impact in Tehran, Iran: *Proceedings of the Climate Change Impacts on Water Resources, Belgrade, Serbia*, 17–18.
- Mosadegh, E., Babaeian, I., 2021, Projection Of Temperature And Precipitation For 2020-2100 For Tehran Region Using Post-processing Of General Circulation Models Output And Artificial Neural Network Approach (arXiv:2109.04619). arXiv. <https://doi.org/10.48550/arXiv.2109.04619>
- Mosadegh, E., Mejia, J., Wilcox, E. M., Rayne, S., 2018, Vehicle Miles Travel (VMT) trends over Lake Tahoe area and its effect on Nitrogen Deposition, A23M-3068.
- Mosadegh, E., Nolin, A. W., 2020, Estimating Arctic sea ice surface roughness by using back propagation neural network, C014-0005.
- Murphy, J.M., Sexton, D.M.H., Barnett, D.N., Jones, G.S., Webb, M.J., Collins M., Stainforth, D.A., 2004, Quantification of modelling uncertainties in a large ensemble of climate change simulations: *Nature*, 430(7001), 768–72.
- Palmer, T. N., Alessandri, A., Andersen,

- U., Cantelaube, P., Davey, M., Délécluse, P., Déqué, M., Díez, E., Doblas-Reyes, F. J., Feddersen, H., Graham, R., Gualdi, S., Guérémy, J.-F., Hagedorn, R., Hoshen, M., Keenlyside, N., Latif, M., Lazar, A., Maisonnave, E., ... Thomson, M. C., 2004, DEVELOPMENT OF A EUROPEAN MULTI-MODEL ENSEMBLE SYSTEM FOR SEASONAL-TO-INTERANNUAL PREDICTION (DEMETER): Bulletin of the American Meteorological Society, 85(6), 853–872. <http://www.jstor.org/stable/26216980>
- Palmer, T. N., Doblas-Reyes, F. j., Hagedorn, R., Weisheimer, A., 2005, Probabilistic prediction of climate using multi-model ensembles: From basics to applications: Philosophical Transactions of the Royal Society B: Biological Sciences, 360(1463), 1991–1998. <https://doi.org/10.1098/rstb.2005.1750>
- Parry, M.L., Canziani, O.F., Palutikof, J.P., van der Linden, P.J., Hanson, C.E., 2007, IPCC, 2007: Climate Change 2007: Impacts, Adaptation and Vulnerability. Contribution of Working Group II to the Fourth Assessment Report of the Intergovernmental Panel on Climate Change. Eds., Cambridge University Press, Cambridge, UK, 976pp.
- Perkins, S. E., Pitman, A. J., Holbrook, N. J., McAneney, J., 2007, Evaluation of the AR4 climate models' simulated daily maximum temperature, minimum temperature, and precipitation over Australia using probability density functions: Journal of Climate, 20(17), 4356–4376. <https://doi.org/10.1175/JCLI4253.1>
- Rahmani, M.A., Zarghami, M., 2013, A new approach to combine climate change projections by ordered weighting averaging operator; applications to northwestern provinces of Iran: Global and Planetary Change, 102, 41–50.
- Raje, D., Mujumdar, P. P., 2010, Reservoir performance under uncertainty in hydrologic impacts of climate change: Advances in Water Resources, 33(3), 312–326. <https://doi.org/10.1016/j.advwatres.2009.12.008>
- Rietveld, M.R., 1978, A new method for estimating the regression coefficients in the formula relating solar radiation to sunshine: Agricultural Meteorology, 19(2–3), 243–52.
- Semenov, M.A., Barrow, E.M., 2002, LARS-WG A Stochastic Weather Generator for Use in Climate Impact Studies; User Manual. Available from: <http://www.rothamsted.ac.uk/mas-models/download/LARS-WG-Manual.pdf>
- Semenov, M. A., Stratonovitch, P., 2010, Use of multi-model ensembles from global climate models for assessment of climate change impacts: Climate Research, 41(1), 1–14. <https://doi.org/10.3354/cr00836>
- Setegn, S. G., Rayner, D., Melesse, A. M., Dargahi, B., Srinivasan, R., 2011, Impact of climate change on the hydroclimatology of Lake Tana Basin, Ethiopia: Water Resources Research, 47(4). <https://doi.org/10.1029/2010WR009248>
- Solomon, S., Qin, D., Manning, M., Chen, Z., Marquis, M., Averyt, K.B., Tignor, M., Miller, H.L., IPCC, 2007: Climate Change 2007: The Physical Science Basis: Contribution of Working Group I to the Fourth Assessment Report of the Intergovernmental Panel on Climate Change: Eds., Cambridge University Press, Cambridge, UK, 996 pp.
- Tebaldi, C., Smith, R. L., Nychka, D., Mearns, L., 2005, Quantifying Uncertainty in Projections of Regional Climate Change: A Bayesian Approach to the Analysis of Multimodel Ensembles: Journal of Climate, 18(10), 1524–40. <https://doi.org/10.1175/JCLI3363.1>



- Tebaldi, C., Knutti, R., 2007, The use of the multi-model ensemble in probabilistic climate projections: *Philosophical Transactions of the Royal Society A: Mathematical, Physical and Engineering Sciences*, 365(1857), 2053–2075. <https://doi.org/10.1098/rsta.2007.2076>
- Wilby, R., Charles, S., Zorita, E., Timbal, B., Whetton, P., Mearns, L.O., 2004, *Guidelines for Use of Climate Scenarios Developed from Statistical Downscaling Methods*. 27.
- Wilby, R.L., Harris, I., 2006, A framework for assessing uncertainties in climate change impacts: Low-flow scenarios for the River Thames, UK: *Water Resources Research*, 42(2). Available from: <https://onlinelibrary.wiley.com/doi/abs/10.1029/2005WR004065>